UNITED STATES
NUCLEAR REGULATORY COMMISSION
WASHINGTON, D. C. 20555

MAR 21 1978

MEMORANDUM FOR: Edson G. Case, Acting Director
Office of Nuclear Reactor Regulation

Robert B. Minogue, Director
Office of Standards Development

FROM: Saul Levine, Director
Office of Nuclear Regulatory Research

SUBJECT: RESEARCH INFORMATION LETTER - #25 - FRAP-S3

REFERENCES:

1. P. E. MacDonald, et.al., "MATPRO-Version 09: A Handbook of Materials Properties for Use in the Analysis of Light Water Reactor Fuel Rod Behavior," TREE-NUREG-1005, December 1976

2. J. Rest, "GRASS-SST: A Comprehensive, Mechanistic Model for the Prediction of Fission-Gas Behavior in UO_2 Base Fuels During Steady-State and Transient Conditions," to be published

This Research Information Letter transmits the FRAP-S3 code description and verification documentation.

Introduction

FRAP-S3 is a best-estimate computer code that calculates the thermal and mechanical response characteristics of a nuclear fuel rod operating under steady-state power conditions. It is the third version of a code developed to provide accurate initial values of fuel-rod parameters for input into transient analysis codes such as FRAP-T and RELAP. It is capable of supplying the hot-state values of such quantities as:

1. stored energy
2. radial temperature distributions at given axial locations
3. total fission gas release
4. rod internal gas pressure and composition
5. clad deformation
6. amount of pellet-clad interaction (PCI)
7. fuel deformation (swelling, densification, relocation, and thermal expansion)
8. fuel-clad gap size and gap conductance
9. clad corrosion and hydriding.

25

All of these quantities are strongly dependent upon the operating history of the rod, and each will have a large effect on the predicted and measured response of a fuel rod during a transient. The code, therefore, has been designed to provide these and other quantities for any given power history as initial conditions to the transient codes. The required material properties such as thermal conductivity, thermal expansion, etc., are obtained from the MATPRO package (reference 1).

The verification of the FRAP-S3 code had two major objectives: (1) to determine the code performance in predicting the available, qualified, experimental data, and (2) to identify those areas that require more sophisticated modeling or more experimental data. For the first time, the code performance and data were analyzed using statistical methods, since sufficient data are now available for significant results. Thus, all of the major response variables are presented along with their corresponding standard error bounds. A statistical spread can now be put on such input as stored energy when computing the behavior of a rod during a transient. The verification procedure used information from over 700 fuel rods containing a wide range of operating and design parameters.

Discussion

Code Description. A typical PWR or BWR fuel rod is divided into a maximum of 15 axial segments, each operating at a power level averaged over its length. It is also divided into a maximum of ten radial rings. Each ring-segment volume element is assumed to possess averaged properties such as temperature and power. The fuel rod power history is approximated by a series of steady-state power levels with instantaneous jumps from one level to another. Five major calculational models are used in the code: thermal, gas pressure, fuel deformation, clad deformation, and fuel-clad interaction. Although these models are interdependent, the calculational techniques used in them are distinct, and can be described separately.

The fuel rod temperature model is based on the following assumptions: (1) there is no axial or circumferential heat conduction, (2) steady-state boundary conditions exist during each power step, and (3) gamma heating effects are negligible. The calculation begins with the determination of the bulk coolant temperature at each axial segment using the standard thermal-hydraulic equation for channel flow, and specifying the needed thermal-hydraulic parameters. The temperature drops between the coolant and rod surface, across the clad oxide layer, and across the cladding are then computed in sequence using the Fourier heat flow law as applied to thin layers. Next, the temperature drop across the

fuel-clad gap is computed. This calculation requires the use of iterative methods since the gap conductance depends strongly on temperature through its two major parameters, gap size and gas thermal conductivity. Each of these parameters depends, in turn, on the other major models of the code through such processes as fission gas release, fuel swelling, fuel densification, fuel relocation, and fuel and clad thermal expansion. As a result, the gap temperature calculation and the subsequent fuel temperature calculation is done within an iteration loop which encloses the calculations of the above phenomena. The fuel pellet temperature distribution is computed using the $\int KdT$ method (see Enclosure 1) in which account is taken of the effects of neutron flux depression on the volumetric heat generation rate.

The fuel rod internal gas pressure model assumes: (1) the perfect gas law inside the rod, (2) gas pressure is constant throughout the rod, and (3) the gas in fuel pellet cracks is at the fuel average temperature. The rod is considered to consist of regions along its axis, each having an average temperature and gas volume determined by the average fuel and clad dimensions over the axial segment. The plenum gas temperature is calculated via convective heat transfer between the plenum gas and its contacting surfaces; i.e., the top of the pellet stack, the holddown spring, and the cladding. Gamma heating is accounted for in the plenum spring. Fission gas production and release are computed using empirical correlation models. Gas production is burnup-dependent only, whereas its release utilizes a correlation equation containing time, temperature, and fuel density.

The fuel rod deformation model contains three submodels: thermal expansion, irradiation-induced swelling, and densification. It, therefore, assumes that no mechanical deformation of the fuel occurs via fuel-clad contact or thermal stresses, and that no fuel creep occurs under applied stress. The thermal expansion model assumes that each fuel ring expands fully in both the axial and radial directions with no constraining influence arising from the circumferential expansion. The fuel swelling model is obtained from MATPRO via a correlation equation dependent on burnup and temperature. The fuel densification calculation is also obtained from MATPRO correlation equations, which relate the density change to the sintering temperature, initial fuel density, and burnup.

The cladding deformation model consists of many submodels which account for time-independent elastic and plastic deformation, and time-dependent plastic deformation (creep). It uses the incremental theory of plasticity and the Prandtl-Reuss flow rule (see Enclosure 1) to determine the plastic strain increments for each set of load conditions; it obtains

the required mechanical properties from MATPRO correlations. The model contains the following assumptions: (1) work-hardening is isotropic; (2) stress, strain, and temperature are uniform through the cladding thickness; (3) no slippage occurs at the fuel-clad interface; (4) bending stresses and strains in the clad are negligible; and (5) the loading and deformation are axisymmetric. In general, the methods used to solve for the stress and strain in the clad depend upon the structural relationships between the fuel and clad at the time of the load step. If the fuel-clad gap is open, the stresses are calculated directly from the stress theory of a thin cylindrical shell with specified internal and external pressures. If the gap is closed, the model used is a thin cylindrical shell with a prescribed external pressure and a prescribed radial displacement of its inside surface. This radial displacement is obtained from the fuel deformation model. Moreover, since no slip is allowed, the axial fuel strain is transmitted directly to the cladding, thereby prescribing the axial strain in the clad. If the gap is partially closed (i.e., pinched off) along the rod axis, a "trapped stack" regime results. The model used in this situation is a thin cylindrical shell with specified internal and external pressures and a prescribed total change in length of the cylinder. Whereas, the first two models solve for the stresses and strains at one axial segment at a time, the trapped stack model simultaneously solves for all the axial segments within the regime. Details of the iteration loops and computational methods used are given in Enclosure 1.

The fuel clad interaction model was developed to predict cladding failure as a result of any of the following phenomena:

1. clad melting
2. oxide layer wall thinning
3. ballooning (without rupture)
4. eutectic melting
5. clad collapse
6. overstress or overstrain failure
7. cumulative stress damage.

Actually, the model consists of several subroutines, each of which computes the probability of failure via one of the above mechanisms. The model then combines these probabilities into a single overall failure probability of the cladding.

Results - Verification of FRAP-S3

As stated earlier, the verification of the FRAP-S3 code utilized data from over 700 fuel rods, encompassing a wide range of operating and

design parameters. The verification effort involved over 700 individual computer runs and extensive statistical analysis of the results. As shown below, the overall performance of FRAP-S3 in predicting the important parameters of the models described above is excellent. Although improvement may be desired in some areas, in other areas the code approaches the limit of accuracy of the experimental data. The code performance in predicting rod temperature, rod pressure, and rod deformation is summarized below.

The thermal performance was analyzed using fuel centerline temperature results of over 100 rods representing over 800 data points. Figures 1 and 2 summarize the results for unpressurized and pressurized rods, respectively. The standard errors between predicted and measured values based on these figures were 198°K and 254°K, respectively. On a percentage basis for a centerline temperature of 1500°K, for example, these results translate to 14% and 17%, respectively. This indicates an accuracy within, or close to, data measurement uncertainty.

The fuel rod pressure performance is summarized in Figure 3 for 48 rods (including both pressurized and unpressurized) and 658 data points. The respective standard errors in the calculated pressure for pressurized and unpressurized rods was 1.34 and 0.66 MPa. The group of underpredictions between pressures of 7.58 and 11.72 MPa corresponds to BOL measurements on two rods which exhibited significant transducer drift. Burnup values ranged from 3000 to 22,000 MWd/MTM. The errors in terms of percentage correspond to ~14% for a pressurized rod operating at 10 MPa, and ~34% for an unpressurized rod operating at 2 MPa. The latter error is reduced to less than 10% if only BOL conditions are used. This reflects the strong influence of gas release on the pressure uncertainty in unpressurized rods.

The fission gas release comparison is shown in Figure 4 for 176 fuel rods. The standard error in the gas release fraction is 0.188 which corresponds to about a 40% error in a rod releasing 50% of its gas. As can be seen from Figure 4, the large overall error is caused by considerable overprediction at the low end (less than 10% release) of the data spectrum. The code performance is much better for high release data. The poor performance at the low end is believed to be caused by inadequate modeling of the diffusion processes occurring at the start of release. It is hoped that the GRASS computer model (reference 2) for gas release, when coupled to the code (either as a fast-running approximate version or as a GRASS-derived correlation equation), will reduce the error considerably.

One of the most important (and most difficult to predict) indicators of the rod deformation model, is the prediction of the heat rating at which gap closure occurs. The performance of FRAP-S3 in this respect is shown in Figure 5 for 77 rods. The horizontal lines indicate the range of data uncertainty. The standard error is 13.4 KW/M, which corresponds to an error of ~50% for a typical PWR rod operating at 26 KW/M (8 KW/ft). Although this uncertainty is not small, it is a considerable improvement over previous versions of the code. The improvement noted here (and also reflected in the thermal performance) is due to a new fuel relocation model coupled with an improved accounting of the effects of relocation-induced cracks on the pellet thermal conductivity. Another measure of the performance of the rod deformation model is the total permanent axial expansion of the fuel stack caused by swelling and densification. Figure 6 shows the code performance in this area for 100 rods and 368 data points. The burnup range in the data sample has been significantly extended over previous versions by inclusion of power reactor post-irradiation examination results. The calculated standard error is 0.44% of the active length. The amount of deformation, though small, is generally underpredicted, since compression effects on the fuel have not been modeled as yet.

Finally, the code performance in predicting the permanent cladding hoop and axial strains is illustrated in Figures 7 and 8. A total of 170 rods containing 393 data points were used in the hoop strain comparison, whereas 115 rods with 161 data points were used for the axial comparison. The computed standard errors were 0.59% of cladding diameter and 0.47% of the active length, respectively. The hoop strain calculations are dominated by the creep collapse model in the code and tend to overpredict the data. The reasons for this may be twofold: the add-on fast-flux term for creep may be too high, or the free-standing clad model used neglects the possible support that the clad can receive from the fuel. The points showing large overpredictions of the axial strain in Figure 8 correspond to small gap or high temperature conditions, under which structural gap closure is calculated. Since no stress-induced fuel deformation is modeled, the cladding strain consequences of gap closure are overestimated. In any event, the measured and predicted strains are quite small and are not expected to have much influence on the effective gap size and corresponding thermal calculations. It has been shown above that the thermal model gives excellent agreement with the data, and that the onset of gap closure is reasonably well predicted; both of these predictions take into account the computed cladding strains.

Table I summarizes the standard errors for the above response characteristics, plus the cladding corrosion and hydriding behavior and axial fuel thermal expansion results.

Recommendations

The above results are offered for user office consideration for application to the identified regulatory need. The information presented herein should be especially useful in the current RSR/NRR Code Coordination effort. The statistical analysis used will aid in the licensing evaluation of the code output, and serve to direct the effort in the development of the evaluation models to be used in the new steady-state FRAPCON code. For information on further evaluation of the results, G. P. Marino of the Fuel Behavior Research Branch of Reactor Safety Research may be contacted.

Saul Levine

Saul Levine, Director
Office of Nuclear Regulatory Research

Enclosures:

Enclosure 1 - J. A. Dearien, G. A. Berna, M. P. Bohn, J. D. Kerrigan and D. R. Coleman, "FRAP-S3: A Computer Code for the Steady-State Analysis of Oxide Fuel Rods, Volume 1 - FRAP-S3 Analytical Models and Input Manual," October 1977, TFBP-TR-164

Enclosure 2 - D. R. Coleman, E. T. Laats and N. R. Scofield, "FRAP-S3 - A Computer Code for Steady-State Analysis of Oxide Fuel Rods, Volume 2 - Model Verification Report," October 1977, TFBP-TR-228

See cc next page

cc w/o Enclosures:
L. Rubenstein, NRR
V. Stello, DOR
D. Ross, DSS
R. Baer, DOR
P. Check, DSS
Z. Rosztoczy, DSS
C. Fitzgerald, MIPC
W. Reinmuth, IE
R. Mattson, DSS
M. Kenemuyi, A/DGES
G. H. Smith, IR
C. MacDonald, FCTR
J. Volgłewede, DSS
R. Lobel, RS

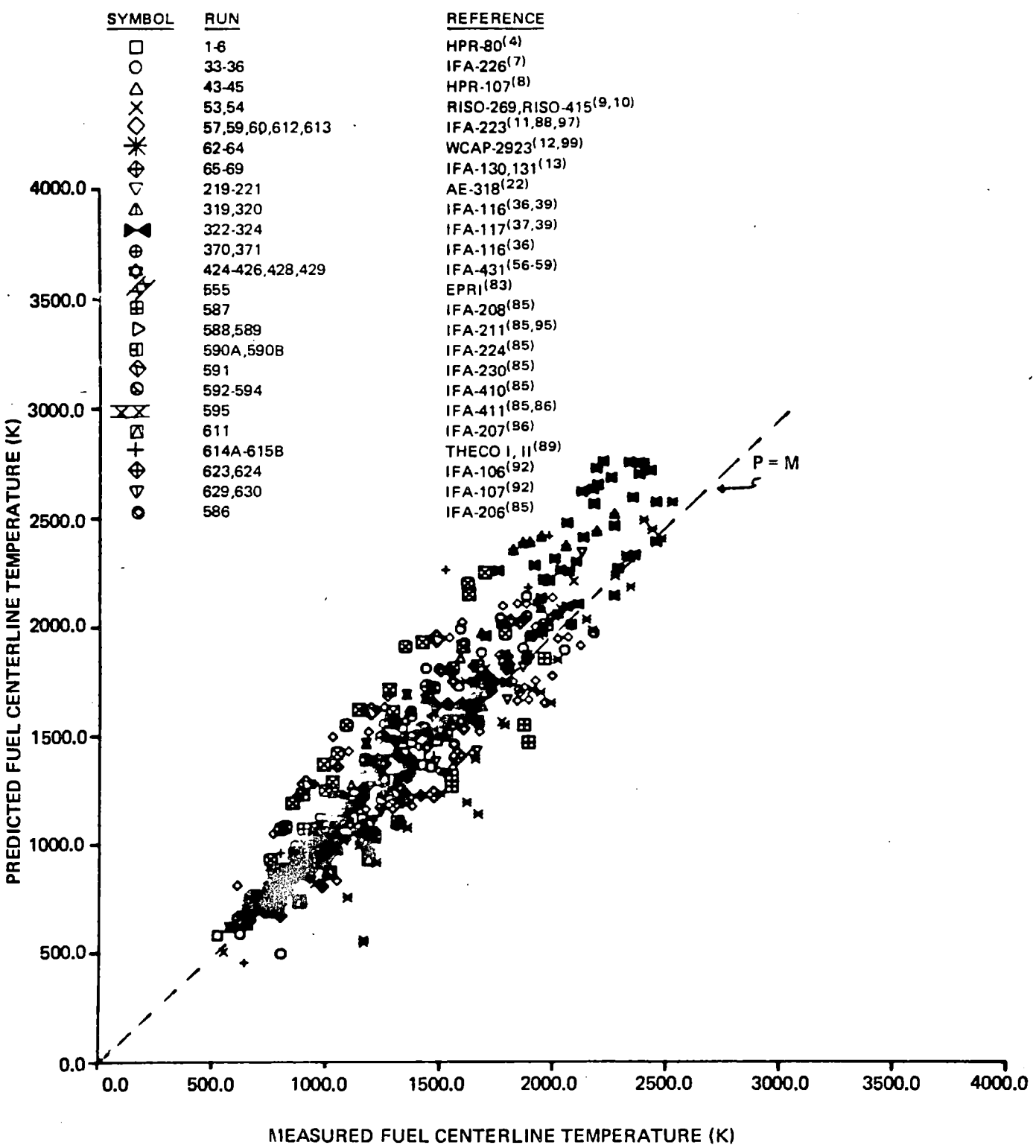

Figure 1. FRAP-S3 Predicted Versus Measured Center Temperatures for Unpressurized Rods.

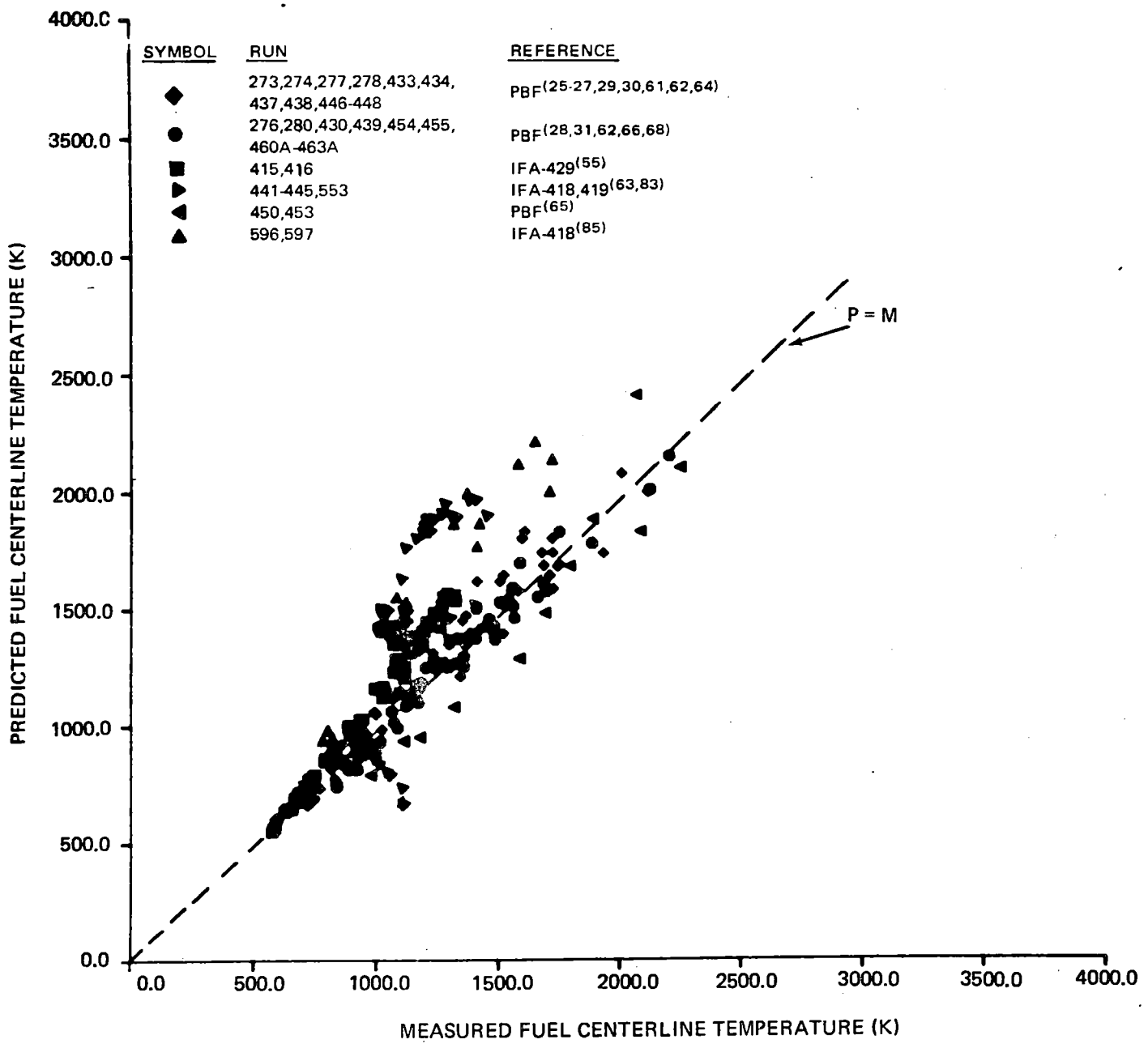

Figure 2. FRAP-S3 Predicted Versus Measured Center Temperatures for Pressurized Rods.

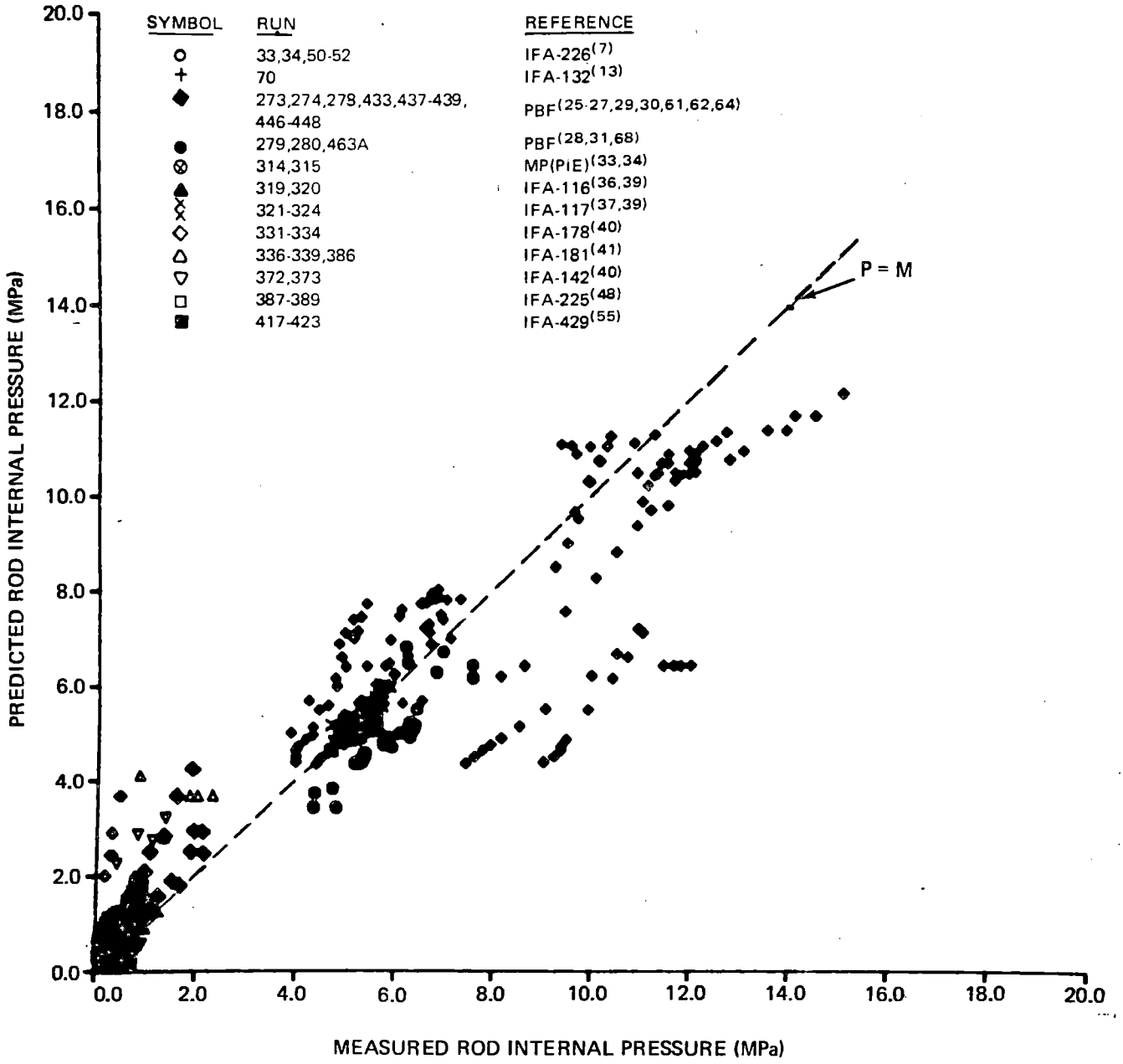

Figure 3. FRAP-S3 Predicted Versus Measured Rod Internal Pressure.

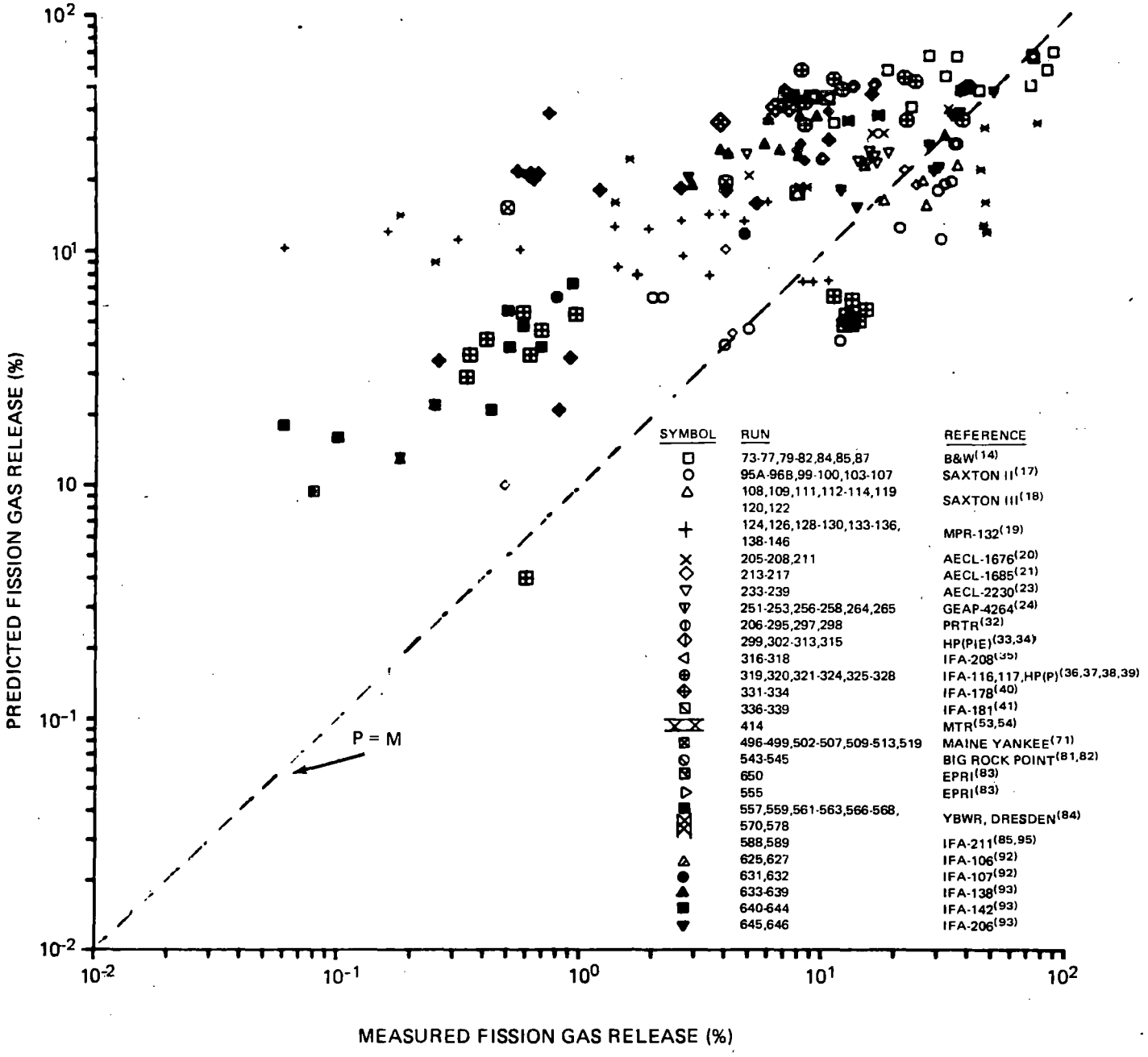

Figure 4. FRAP-S3 Predicted Versus Measured Fission Gas Release Fraction.

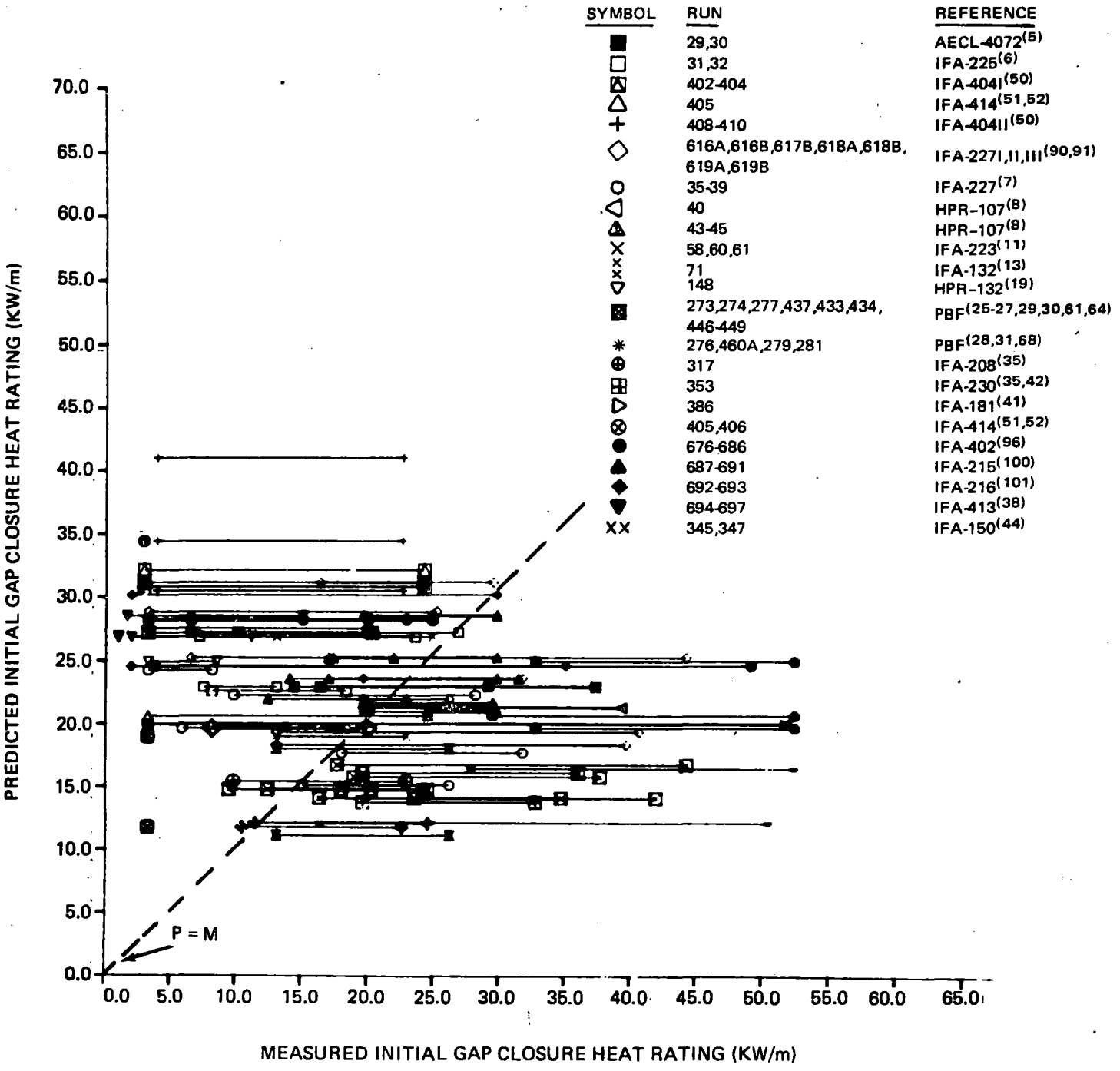

Figure 5. FRAP-S3 Predicted Versus Measured Gap Closure Heat Rating

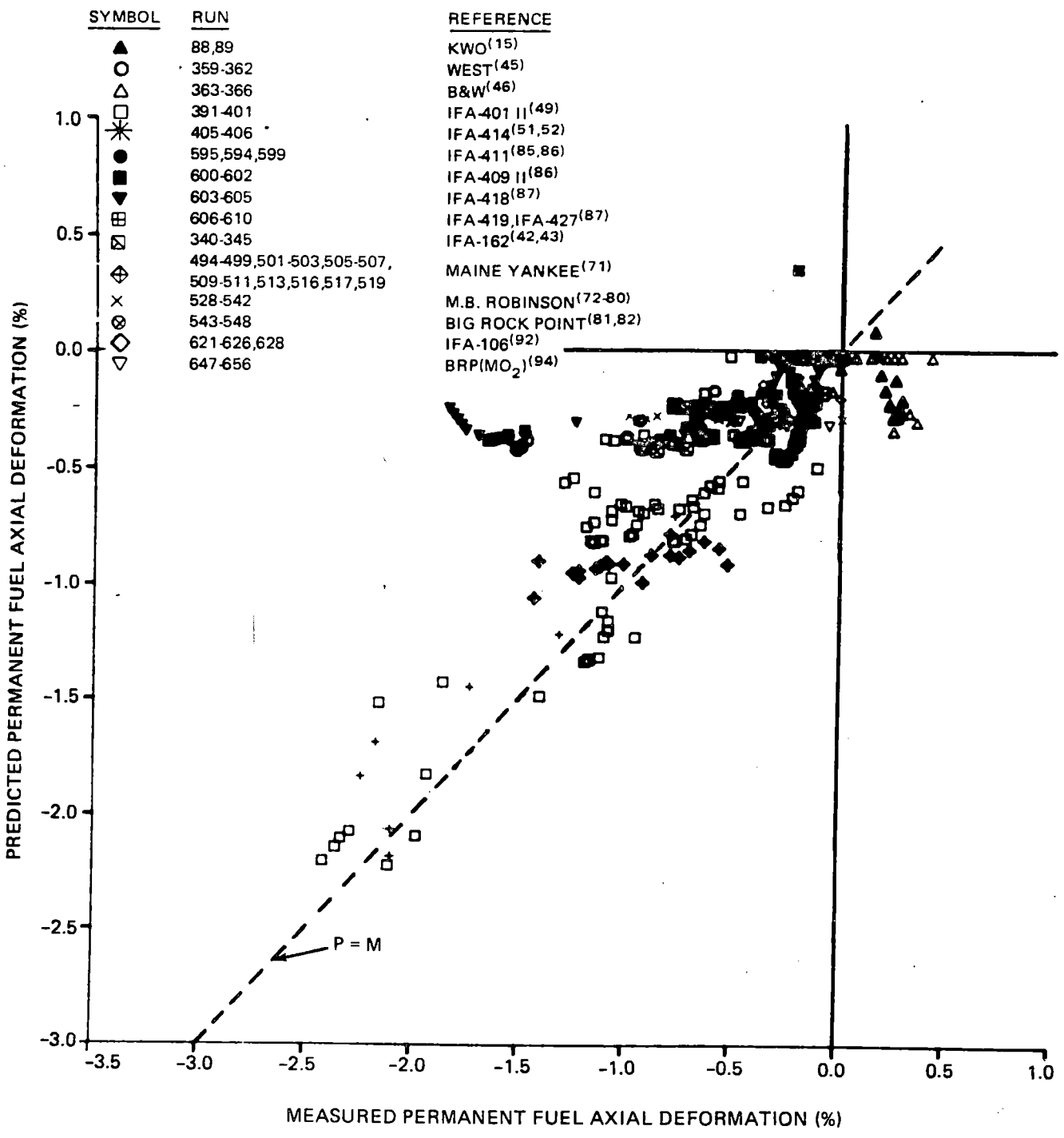

Figure 6. FRAP-S3 Predicted Versus Measured Permanent Fuel Axial Deformation

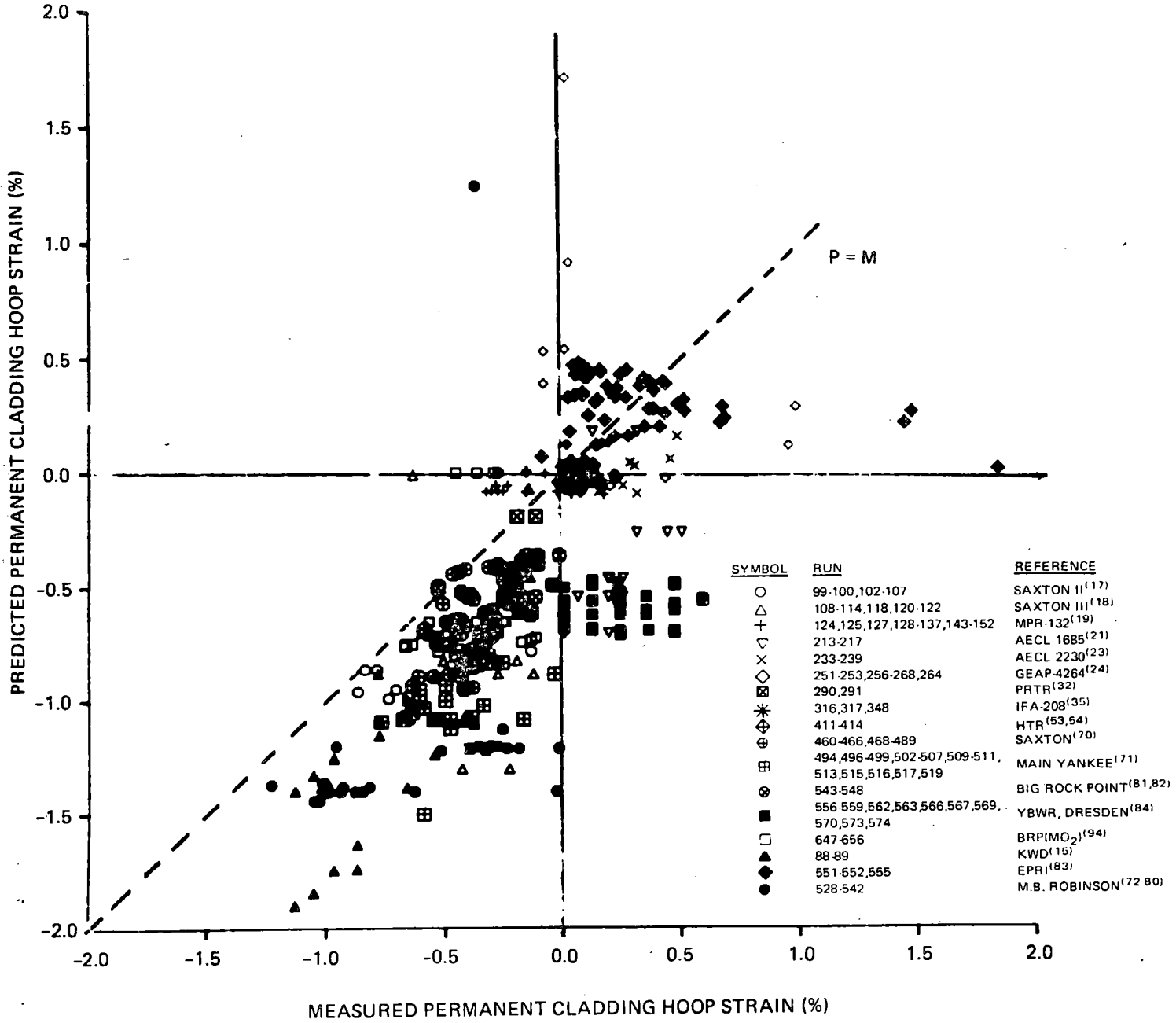

Figure 7. FRAP-S3 Predicted Versus Measured Permanent Cladding Hoop Strain

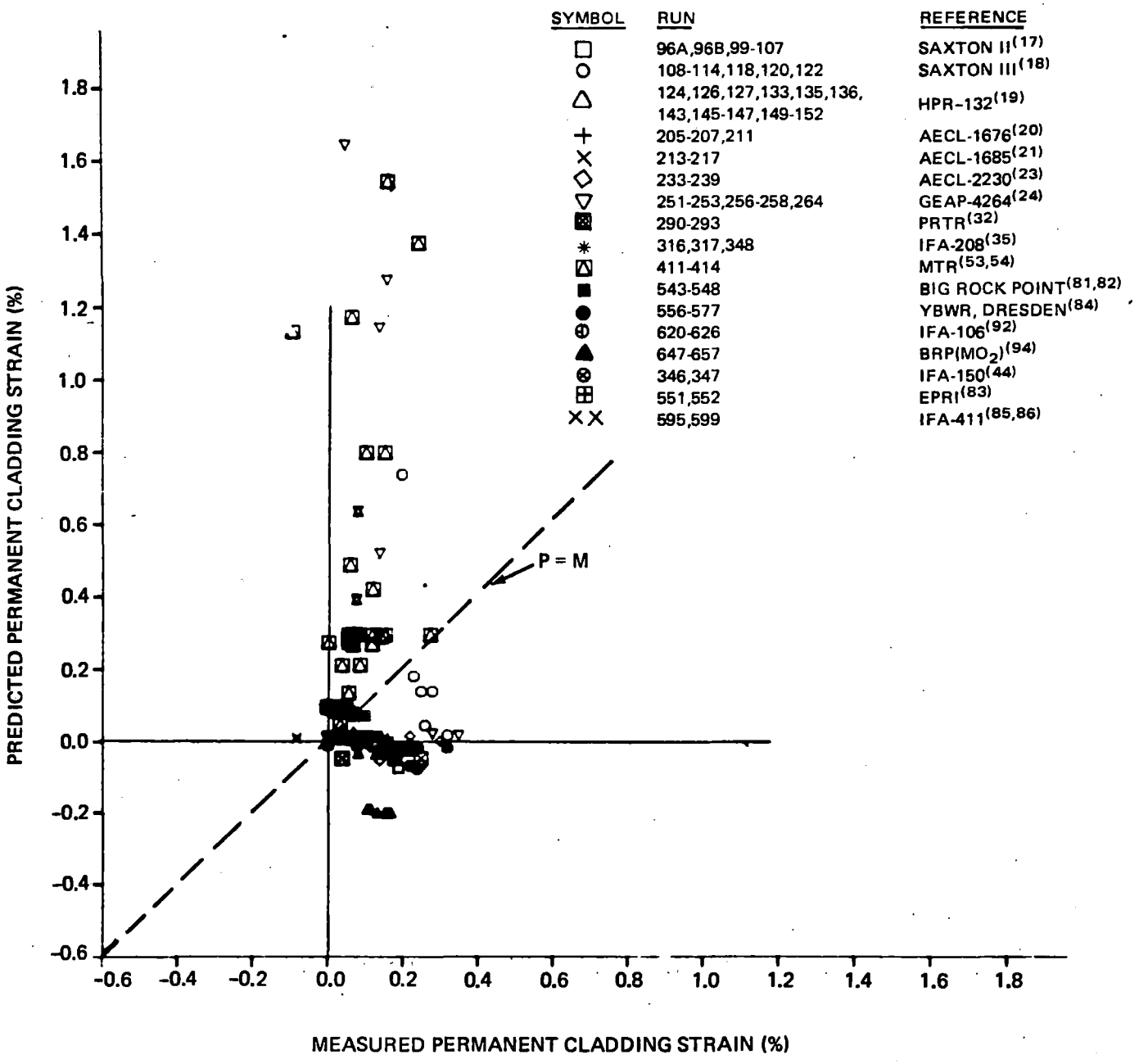

Figure 8. FRAP-S3 Predicted Versus Measured Permanent Cladding Axial Strain.

TABLE I

FUEL BEHAVIOR VERIFICATION: FRAP-S3
STANDARD ERROR SUMMARY

Output Parameter	Sample Size (Rod/Pts)	Standard Error
Fuel Center Temperature	33/290 64/511	254 K (Pressurized Rods) 198 K (Unpressurized Rods)
Released Fission Gas	176/176	18.8% Generated Gas
Rod Internal Pressure	28/309 20/349	0.66 MPa (Unpressurized) 1.34 MPa (Pressurized)
Gap Closure Heat Rating	77/77	13.4 KW/m
Axial Fuel Thermal Expansion	19/173	0.37% Active Length
Permanent Fuel Axial Deformation	100/368	0.44% Active Length
Permanent Cladding Hoop Strain	170/393	0.59% Cladding Diameter
Permanent Cladding Axial Strain	115/161	0.47% Active Length
Cladding Surface Corrosion Layer	48/84	6.6μ
Cladding Hydrogen Concentration	38/53	39 PPM